ISSN 0036-0244, Russian Journal of Physical Chemistry A, 2024, Vol. 98, No. 6, pp. 1211–1221. © Pleiades Publishing, Ltd., 2024.
ISSN 0036-0244, Russian Journal of Physical Chemistry A, 2024. © Pleiades Publishing, Ltd., 2024.

STRUCTURE OF MATTER AND QUANTUM CHEMISTRY

Nature of the Lithium Bond in $H_3N\cdots LiHal$ Complexes (Hal = F, Cl, Br) from Quantum Chemical Calculations

A. N. Isaev[a,*]

[a] *Zelinsky Institute of Organic Chemistry, Russian Academy of Sciences, Moscow, 119991 Russia*

**e-mail: isaevaln@ioc.ac.ru*

Received June 13, 2023; revised October 29, 2023; accepted November 1, 2023

Abstract—Properties of lithium- and hydrogen-bonded complexes formed by ammonia molecules, lithium halides (LiHal, A-complexes), and hydrogen halides (HHal, B-complexes) are aligned using quantum chemical MP2/aug-cc-pVTZ calculations. NBO analysis shows energy $E(2)$ of inter-orbital interaction between the monomers grows upon the transition to heavier and less electronegative halogen, along with an increase in the contribution from the *p*-orbital to the hybrid orbital of lithium atom in A-complexes and the hybrid orbital of the halogen atom in B-complexes. The calculated value of $E(2)$ correlates to the elongation of covalent Li–Hal and H–Hal bonds as the complex forms. Analytical investigation of the topology of electron density predicts noteworthily higher values of the electron and potential energy densities at the critical point of intermolecular contact in B-complexes, relative to A-complexes, and a growing mutual penetration of atoms that form the intermolecular contact. The higher thermodynamic stability of lithium-bonded complexes could be due to the stronger positive electrostatic potential on the lithium atoms in molecules of lithium halides and the weaker exchange repulsion of the monomers that form an A-complex.

Keywords: noncovalent interactions, electrostatic potential, lithium and hydrogen bond, polarization energy, MP2/aug-cc-pVTZ calculations

DOI: 10.1134/S0036024424700146

INTRODUCTION

In recent decades, intensive research on the nature of intermolecular interactions has identified several types of noncovalent bonding of molecules. In addition to hydrogen bonds [1], concepts of dihydrogen bonds [2, 3], halogen bonds [4–6], chalcogen bonding [7, 8], pnictogen bonding [9–11], and tetrel bonding [12, 13] have been introduced. Studies of the noncovalent interactions with the participation of elements of the main groups of the Periodic Table should establish a standardized classification. According to the authors of [14], in which this problem was discussed, developing a unified theory of intermolecular interactions will greatly expand chemists' visions of chemical bonding.

It is therefore important to study lithium bond $Y\cdots Li-X$ [15], which remains the one least studied. The lithium (Li-) bond could play an important role in the formation of intermediates and the transition state when conducting reactions of organometallic synthesis. Its study therefore remains pertinent for both theoretical and experimental chemistry. Although the first stage of work on the lithium bond dates back to the 1980s [16–18], the question of its nature is still poorly studied [19]. It is still a matter of debate whether the Li bond can be categorized as a version of the σ-hole bond, the concept of which emerged in theoretical studies of noncovalent interactions with the participation of atoms of group IV–VII elements [20–22].

In the literature, the σ-hole [20] was defined as a region of low electron density that appears as the result of it outflowing upon the extension of the covalent σ bond during the formation of a bond between a IV–VII group atom and a more electronegative atom. The positive electrostatic potential (ESP) is associated with the region of low electron density. Interaction between the positive ESP-potential of the electron-deficient σ-hole region and the donor of the lone unshared pair results into electrostatic stabilization of the molecular complex.

As was noted in earlier theoretical studies [17], the energy of the lithium bond in neutral molecular complexes is much higher than that of the hydrogen (H–) bond and other known noncovalent σ-hole interactions. However, quantum chemical calculations of lithium-bonded complexes were made in the past using relatively small basis sets. Since it is known that a basis set can strongly influence the calculated characteristics of a complex, it is important to study lithium-bonded complexes (especially their geometry and energetics) by modern quantum chemical means. In this work, quantum chemical calculations were made using the Dunning and Pople extended basis sets.

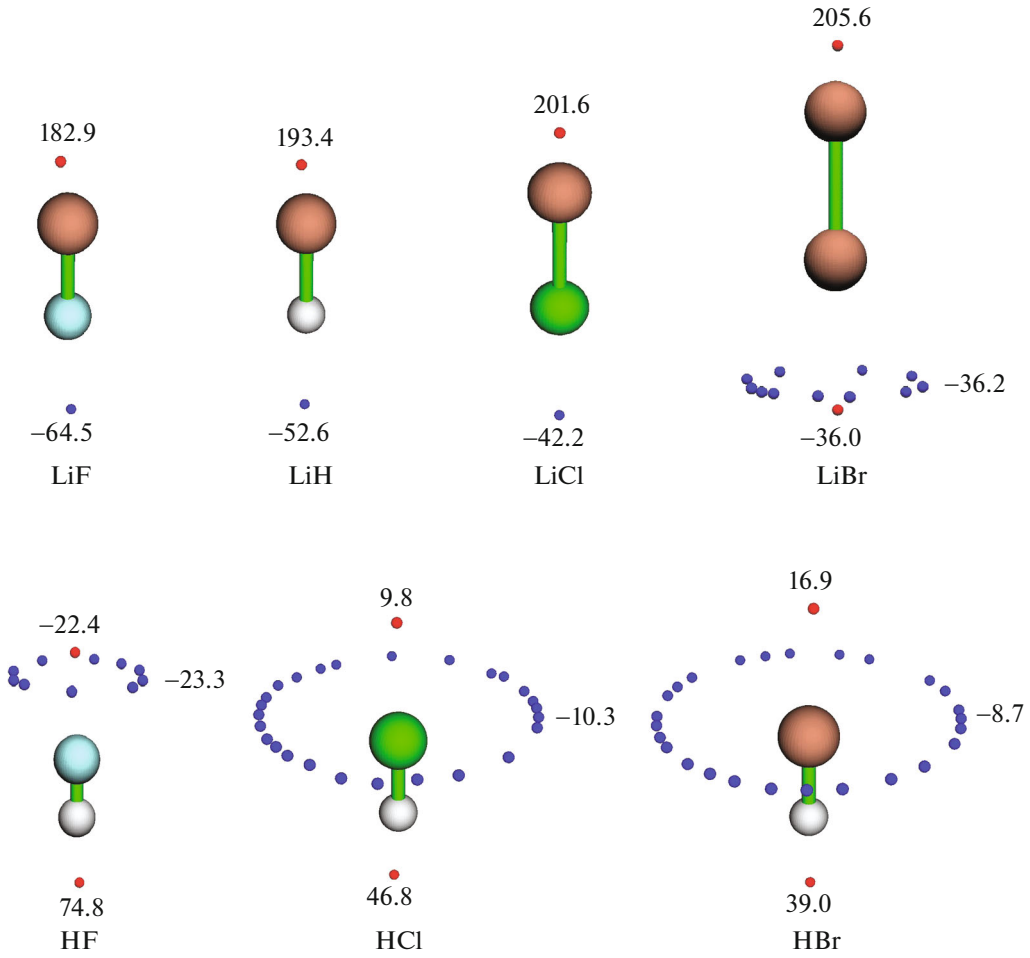

Fig. 1. Positions of maxima of positive electrostatic ESP-potential (red spheres) on van der Waals molecular surface (0.001 a.u. isoline). The numbers show the values of ESP in kcal/mol.

It is known that σ-hole interaction is highly sensitive to the distribution of electron density in a molecule that acts as Lewis acid. It is obvious that we can analyze the effect the deficit of electron density on a Li atom (i.e., the size of a σ-hole) has on the properties of lithium-bonded complexes by varying the electronegativity of a substituent on a lithium atom. The most convenient way of solving this question is to use molecules of lithium halides LiHal as a Lewis acid, which would allow us to see how the properties of a Li bond change along with the electronegativity of halogen bound covalently to a Li atom.

In this work, were compare results from quantum chemical calculations of molecular complexes formed by lithium halides and ammonia molecules to data estimated for similar H-bonded complexes. This kind of comparative analysis is often done in studies of noncovalent interactions because the hydrogen bond [23] is the most studied intermolecular σ-hole interaction. The existence of a region of positive ESP potential on the hydrogen atom and the electrostatic nature of the hydrogen bond [24] were suggested as far back as 1977. It was therefore of interest to compare the maxima of the positive ESP potential on the van der Waals surfaces of LiHal and HHal molecules (Fig. 1).

We can see in Fig. 1 that the effect the halogen atom has on the ESP potential in molecules of lithium halides and hydrogen halides varies. In HHal molecules, the positive potential on the hydrogen atom falls predictably upon moving from the less electronegative halogen of the HF > HCl > HBr series. We see a reverse counter-intuitive trend for lithium halides: the positive ESP-potential grows in the LiF < LiH < LiCl < LiBr series. In addition, the ESP potential on the Li atoms in the LiHal molecules is 3–4 times stronger than the one on the H atoms in the HHal molecules. This agrees with the concept that the deficit of electron density in the region of a σ-hole grows upon moving from light to heavier atoms in the Periodic Table [25]. The higher polarizability and lower electronegativity of a lithium atom relative to hydrogen results into more positive ESP values.

Earlier works on the development of noncovalent interactions showed the prominent role of orbital charge-transfer interactions [26, 27] and dispersive interactions [28, 29] in intermolecular bonding. The aim of this work was to analyze the nature of the Li bond in $H_3N\cdots LiHal$ complexes, based on data from NBO analysis, the topology of electron density, and the decomposition of intermolecular energy into its components.

CALCULATIONS

Our quantum chemical calculations of binary molecular complexes formed by ammonia together with LiHal and HHal (Hal = halogen atom) molecules were made with the Gaussian 09 software [30] according to the MP2 method [31] of the second-order Møller–Plesset perturbation theory. The calculations were made using Dunning's correlation-consistent aug-cc-pVTZ basis set augmented by diffuse functions [32], which has been used extensively in recent years to study noncovalent interactions. Structures obtained in calculations with full optimization of their geometry were checked for the absence of imaginary frequencies in the force constant matrix. To analyze the effect a type of basis functions has on the calculated characteristics of molecular complexes, the geometry and binding energy of the compexes were also calculated using Pople's extended basis set 6-311++G(3*df*,3*pd*) [33].

The bond energies in molecular complexes were defined as the difference between the total energy of a complex and the sum of total energies of the isolated monomers, with allowance for zero point energy. The appropriate procedures of the Gaussian 09 software package were used to analyze the natural bond orbitals (NBO) [34, 35] and NMR chemical shields according to GIAO [36, 37]. Molecular graphs of binary complexes and maps of the electrostatic potential of the LiHal and HHal molecules were constructed on the basis of data from quantum chemical calculations made with the Multiwfn program [38]. We studied the topology of the electron density in complexes according to Bader's theory [39, 40] using the AIM algorithm included in the Gaussian 09 and Multiwfn programs. The intermolecular energy of the monomers forming the lithium- and hydrogen-bonded complexes was decomposed into its components using the GAMESS software package [41, 42].

RESULTS AND DISCUSSION

Geometry and Binding Energy

The calculated geometries of binary lithium-bonded complexes $H_3N\cdots LiHal$ (Hal = F, Cl, Br) (A-complexes) and $H_3N\cdots HHal$ hydrogen-bonded complexes (B-complexes) are presented in Fig. 2 and Table 1. Both types of complexes have *C*3*v* symmetry. Valency angle HNH is a bit greater in the B-complexes, testifying to the flatter umbrella of the ammonia molecule. It is clear from the table that the calculated characteristics of the complexes found using the aug-cc-pVTZ and 6-311++G(3*df*,3*pd*) basis sets are very close. Compared to results from calculations made earlier [16, 17] with the 6-31G(*d*,*p*) basis set, we can see that expanding Pople's basis set greatly reduces the calculated binding energy.

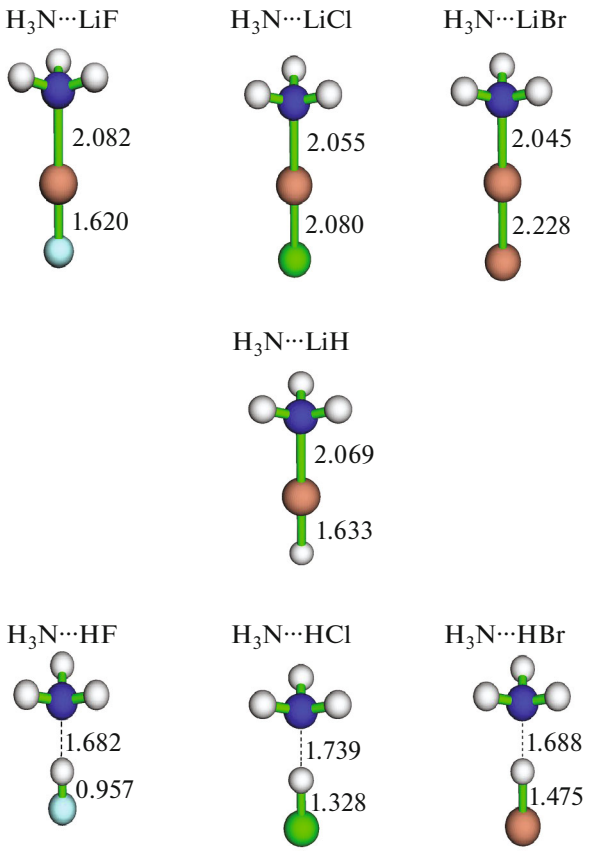

Fig. 2. Binary molecular lithium-bonded complexes (complexes A) and hydrogen-bonded complexes (complexes B).

Our calculations showed that the Li bonds in the studied complexes were centrosymmetrical (unlike those of the H-bonded complexes), and the energy of lithium bonds was more than double that of hydrogen bonds. The change in the energy of lithium bonds in complexes $H_3N\cdots LiHal$ upon varying the halogen substituent in the LiHal molecule reflects the trend of an increase in the positive ESP potential on the Li atom upon reducing the electronegativity of halogen atom. The lowest energy of Li bonds we see is in complex $H_3N\cdots LiF$, and the highest is in the $H_3N\cdots LiBr$ complex. The opposite is true for H-bonded complexes. As Fig. 3 shows, there is a linear correlation between the binding energy and magnitude of the positive ESP potential on the van der Waals surfaces of the

Table 1. Intermolecular distance N···Li/N···H (R), covalent Li–Hal/H–Hal bond length (r), elongation of the covalent Li–Hal/H–Hal bond (Δr) at complex formation, frequency shift ($\Delta\nu$) of the band of stretching vibrations Li–Hal/H–Hal in IR-spectrum, chemical shift (δ) on Li/H atom, valency angle HNH (α) in ammonia molecule, positive electrostatic potential (ESP) on the Li/H atom in Li–Hal/H–Hal molecule and binding energy (E_{bind}) in the lithium- and hydrogen-bonded complexes

Molecular complex	R, Å	r, Å	Δr, mÅ	$\Delta\nu_{Li-Hal/H-Hal}$, cm^{-1}	δ_{Li}/δ_H, ppm	α(HNH), deg	ESP, kcal/mol	E_{bind}, kcal/mol	
								without ZPE	with ZPE
Complex A: lithium bonds									
$H_3N\cdots LiF$	2.082 (2.084)	1.620 (1.618)	26.1 (26.5)	−1.3 (−1.1)	−0.35 (−0.16)	106.1 (106.5)	182.9 (183.3)	19.64 (19.85)	17.68 (17.83)
$H_3N\cdots LiCl$	2.055 (2.058)	2.080 (2.073)	31.3 (31.3)	59.0 (54.4)	−0.92 (−0.53)	106.1 (106.5)	201.6 (202.1)	22.09 (22.33)	20.07 (20.36)
$H_3N\cdots LiBr$	2.045 (2.052)	2.228 (2.234)	31.5 (33.8)	91.9 (82.1)	−0.90 (−0.47)	106.1 (106.6)	205.6 (204.9)	23.12 (22.82)	21.09 (20.85)
$H_3N\cdots LiH$	2.069 (2.072)	1.633 (1.633)	27.7 (30.0)	−71.3 (−68.9)	−1.69 (−1.35)	106.2 (106.4)	193.4 (193.8)	19.89 (19.99)	17.67 (17.77)
Complex B: hydrogen bonds									
$H_3N\cdots HF$	1.682 (1.683)	0.957 (0.951)	34.9 (34.4)	−790.6 (−779.3)	−7.30 (−6.95)	107.3 (107.8)	74.8 (75.2)	12.93 (13.10)	9.90 (9.90)
$H_3N\cdots HCl$	1.739 (1.740)	1.328 (1.324)	52.7 (51.9)	−742.9 (−735.6)	−10.27 (−9.74)	107.4 (107.9)	46.8 (46.1)	9.22 (9.08)	6.93 (6.80)
$H_3N\cdots HBr$	1.688 (1.717)	1.475 (1.477)	68.7 (64.0)	−858.5 (−853.2)	−12.33 (−11.47)	107.7 (108.4)	39.0 (37.9)	9.01 (8.05)	6.85 (5.94)

Data from MP2/6-311++G(3*df*,3*pd*) calculations of complexes are in parentheses.

LiHal and HHal molecules for the complexes of both types. It is interesting that the binding energies in complexes $H_3N\cdots LiF$ and $H_3N\cdots LiH$ are virtually the same, according to our calculations.

GIAO calculations of the NMR chemical shifts on atoms in complexes A and B predicted values of δ_H an order of magnitude higher than those of δ_{Li}. We can see from Table 1, which presents calculated values of

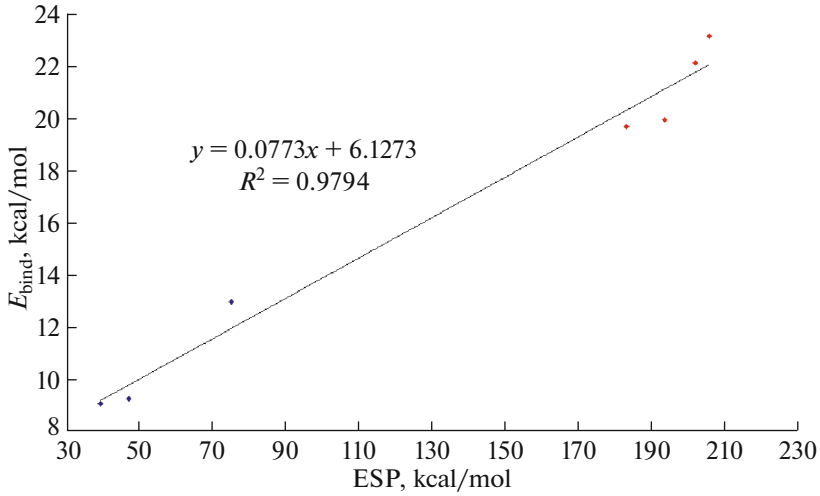

Fig. 3. Linear correlation between a magnitude of electropositive ESP-potential on a van der Waals surface of LiHal and HHal molecules and binding energy E_{bind} in molecular lithium-bonded complexes (red diamond symbol) and hydrogen-bonded complexes (blue diamond symbol).

Table 2. Percentage contribution of *p*-orbital (*%p*) to hybrid orbitals, NPA-occupation (η) of orbital, change in the charge (Δq) on the atoms as the complex forms, charge (Q_{tr}) transferred from ammonia molecule, and energy of second-order perturbation ($E(2)$) in the lithium- and hydrogen-bonded complexes

Molecular complex	n_N-orbital		$n^*_{Li}/\sigma^*_{H-Hal}$		Δq, me			Q_{tr}, me	$E(2)$, kcal/mol
	%p	η	*%p*	η	Δq_N	$\Delta q_{Li}/\Delta q_H$	Δq_{Hal}		
Complex A: lithium bonds									
$H_3N\cdots LiF$	76.81 $sp^{3.31}$	1.9670	9.27 $sp^{0.10}$	0.0307	−49.5	−53.8	21.0	32.8	17.94 (4.44)
$H_3N\cdots LiCl$	77.17 $sp^{3.38}$	1.9542	49.92 $sp^{1.00}$	0.0499	−42.7	−97.2	48.1	49.1	33.40 (13.40)
$H_3N\cdots LiBr$	77.29 $sp^{3.41}$	1.9522	53.24 $sp^{1.14}$	0.0539	−42.0	−107.3	55.2	52.1	34.95 (15.95)
$H_3N\cdots LiH$	77.29 $sp^{3.41}$	1.9541	69.85 $sp^{2.34}$	0.0420	−34.7	−108.4	58.9	49.5	26.38 (12.15)
Complex B: hydrogen bonds									
$H_3N\cdots HF$	77.20 $sp^{3.39}$	1.9394	71.42 $sp^{2.51}$	0.0568	−4.1	22.1	−78.8	56.6	40.87
$H_3N\cdots HCl$	77.17 $sp^{3.38}$	1.9236	80.01 $sp^{4.13}$	0.0716	11.6	61.3	−132.0	70.7	43.35
$H_3N\cdots HBr$	77.35 $sp^{3.42}$	1.9027	82.33 $sp^{4.79}$	0.0926	23.1	77.1	−167.9	90.8	55.24

Numbers in parentheses in the last column of Table 2 gives the values $E(2)$ for interaction of n_N-orbital of lone-electron pair of nitrogen atom and anti-σ-orbital of covalent bond Li−Hal upon the formation of lithium-bonded complexes.

chemical shifts to the low-frequency region, that the shielding of nuclei of hydrogen and lithium atoms gets weaker upon moving to heavier and less electronegative halogen.

An atypical picture of the elongation of the covalent bond in the lithium halide molecule is observed upon the formation of Li-bonded complexes A, which is accompanied by frequency ν_{LiHal} of Li−Hal shifting into the short-wave region. The blue shift of the IR-band in lithium-bonded complexes has also been noted in experimental and theoretical works (e.g., [18, 43, 44]). It should be noted that the shift of the IR band of HX to short-wave frequencies during the formation of H-bonded complexes was noted in the literature only when the corresponding covalent bond was shortened. The band shifts to the long-wave area during the formation of H-bonded complexes when it is elongated.

In the literature, a numerous ideas were expressed to explain the character of the change of the X−H covalent bond length (i.e., its elongation and shortening as a complex forms [45–48]). According to data from the quantum chemical study in [47], the behavior of the X−H covalent bond in H-bonded Y···H−X complexes is determined by the ratio of contributions from hyperconjugation $n(Y)$, $\sigma^*(X-H)$ and the rehybridization of heteroatom X. The X−H bond grows longer when hyperconjugation predominates, but the covalent bond can be shortened when there is a marked increase in the *s*-character of the hybrid orbital of heteroatom X. We studied this problem after analyzing the natural orbitals (NBOs) of complexes A and B as described in the next section.

Analyzing Natural Bond Orbitals (NBOs) (NBO Analysis)

An analysis of NBOs according to data from MP2/aug-cc-pVTZ calculations of complexes A and B shows obvious differences in the inter-orbital interaction between monomers upon the formation of lithium and hydrogen bonds (Table 2). The interaction between the *n*-orbital of the lone-electron pair of the nitrogen atom and the anti-σ-orbital of the H−Hal covalent bond ($n_N \rightarrow \sigma^*_{H-Hal}$) responds to the formation of H bonds, while the overlapping of the *n*-orbital of nitrogen and the anti-orbital of the lone pair of lithium atom ($n_N \rightarrow n^*_{Li}$) makes the major contribution to the energy of inter-orbital interaction upon the formation of Li bonds. Interaction $n_N \rightarrow \sigma^*_{Li-Hal}$, like the $n_N \rightarrow \sigma^*_{H-Hal}$ of monomers in complexes B, is much less with the lithium bond. It is therefore obvious from Table 2 that the calculated energy of second-order perturbation $E(2)$ for interaction $n_N \rightarrow n^*_{Li}$ in complex $H_3N\cdots LiCl$ is 33.4 kcal/mol. The value of $E(2)$ is 13.4 kcal/mol for interaction $n_N \rightarrow \sigma^*_{Li-Cl}$.

We can see from Table 2 that Bent's rule applies to A-complexes [49]. Under the rule, the *p*-character of hybrid orbital of atom rises as the electronegativity of the substituent covalently bound to this atom falls. We can see the smallest contribution from the *p*-component to the hybrid orbital of the lithium atom in the LiF molecule, while the largest contribution is in the LiBr molecule. In the complexes A, energy $E(2)$ of inter-orbital interaction rose along with the contribution from the *p*-orbital to the hybrid orbital of the Li

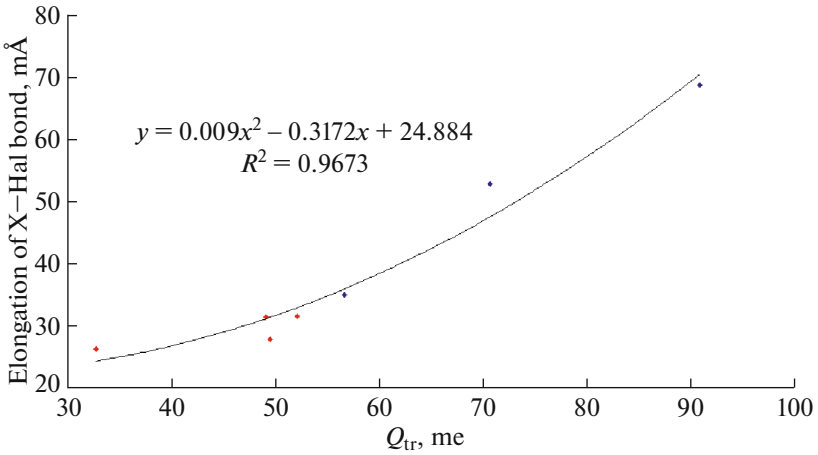

Fig. 4. Correlation of magnitude of charge Q_{tr} transferred to Lewis acid, and elongation of the covalent X–Hal bond (X = Li, H) at formation of the lithium-bonded complexes (red diamonds) and hydrogen-bonded complexes (blue diamonds).

atom. A linear dependence of energy $E(2)$ of interorbital interaction $n_N \rightarrow \sigma^*_{Li-C}$ and the percentage of the contribution from the *p*-component to the hybrid orbital of lithium was found in [19] while studying lithium-bonded complexes N···Li–C formed by ammonia molecules and lithium-substituted hydrocarbons. Note that Table 2 shows a similar pattern of the symbate change in the value of $E^{(2)}_{n_N \rightarrow \sigma^* H-Hal}$ for B-complexes when the *p*-component of the hybrid orbital of the halogen atom participating in the formation of covalent bond H–Hal was altered.

The predominant mode of interorbital overlapping determines the pattern of charge transfer from the ammonia molecule. In Li-bonded complexes, the electronic charge is mostly transferred to the lithium atom, which was acknowledged theoretically in [18, 50, 51], but charge is transferred to the halogen atom in H-bonded complexes. The calculated values of the change in the NPA charges on the atoms in complexes A and B are given in Table 2, which shows that increased inter-orbital interaction between the monomers in the complexes with heavy halogen strengthened the electron charge transferred to the LiHal and HHal molecules. Figure 4 also shows that charge Q_{tr} transferred from ammonia correlates well with the elongation of the covalent Li–Hal and H–Hal bonds in both types of complexes.

The elongation of covalent bonds testifies to the predominance of hyperconjugation over the rehybridization of atoms in the molecules of lithium halides and hydrogen halides upon the formation of Li- and H-bonded complexes. An increase in energy $E(2)$ of inter-orbital interactions $n_N \rightarrow \sigma^*_{Li-Hal}$ and $n_N \rightarrow \sigma^*_{H-Hal}$, i.e. a strengthening of hyperconjugation, has been noted in complexes A and B with a weakening of the electronegativity of the halogen). The energy of hyperconjugation is several times higher in B-complexes than in A-complexes, which apparently determines the notably greater lengthening of the covalent H–Hal bonds, relative to the Li–Hal bonds.

Topological Analysis

Figure 5 presents molecular graphs of complexes H_3N···LiCl and H_3N···HCl, constructed on the basis of analyzing the topology of electron density according to MP2/aug-cc-pVTZ calculations, which demonstrate the existence of an intermolecular bond path connecting the nitrogen atoms to the lithium and hydrogen atoms. Values of the topological parameters of the bond critical points BCP (3, −1) of intermolecular contact N···Li and N···H, found according to Bader's Theory of Atoms in Molecules (AIM) [39, 40], are given in Table 3. It should be noted that the topological parameters of the critical point are considered important indicators of intermolecular interaction. For example, it is clear from the table that the Laplacian of electron density $\nabla^2\rho_{BCP}$ at the bond critical point (3, −1) is positive in both types of complexes, which is characteristic of the closed shell systems.

However, analysis of the data in Table 3 shows that Bader's theory fails to explain the markedly higher thermodynamic stability of the Li-bonded complexes, relative to the H-bonded complexes. High values of electron density ρ_{BCP} at the critical point are therefore always viewed as an indicator of higher intermolecular bond strength in [52, 53]. However, the values of ρ_{BCP} in complexes A are about half those in complexes B. The values of potential energy density V_{BCP} and the ELF and LOL localization parameters of electrons and orbitals at the critical point are also notably higher in the latter. The magnitudes of total energy density H_{BCP} in B-complexes are negative, testifying to the covalent component of the intermolecular hydrogen

bond [54]. We would therefore expect stronger bonding of the monomers. The electrostatic ESP potential at the critical points of intermolecular contact N···Li and N···H in studied complexes A and B had similar positive values.

The mutual penetration of the atoms that form this bond is considered to be another index of the strength of intermolecular bonds. In our A-complexes, they were nitrogen and lithium atoms; in the B-complexes, they were nitrogen and hydrogen atoms. The penetration of the atoms can be determined by comparing nonbonded atomic radii r^0 to corresponding bonded atomic radii r. The values of r^0 are determined as the distance from the nucleus to the isoline of electron density (it is usually the isoline of 0.001 a.u.) in the direction of the intermolecular bond, while the value of r is the distance from nucleus to the critical point (3, −1) of the intermolecular contact. By definition, penetration of atoms is the difference between the nonbonded and bonded atomic radii, $\Delta r = r^0 - r$. Table 4 presents the corresponding values of r^0 and r radii for lithium, hydrogen, and nitrogen atoms in complexes A and B, along with calculated values of penetration Δr of atoms during the formation of a complex. It is clear from the table that the mutual penetration of atoms grows along with the transition to heavier halogen in both types of complexes, and the values of Δr_H of hydrogen atom notably higher than those of Δr_{Li} for lithium. According to estimated values of Δr of the atoms of intermolecular bonds and the topological parameters of a bond's critical point, we would expected the bonding of monomers in B-complexes to be stronger than in A-complexes.

It is interesting to compare patterns of the electron shift upon the formation of complexes. Maps of the shift in electron density plotted for complexes $H_3N\cdots LiCl$ and $H_3N\cdots HCl$ are shown in Fig. 6. We can see from the figure that the shifts in electron density upon the formation of hydrogen- and lithium-bonded complexes are in many ways similar, but some quantitative differences should be noted. The loss of

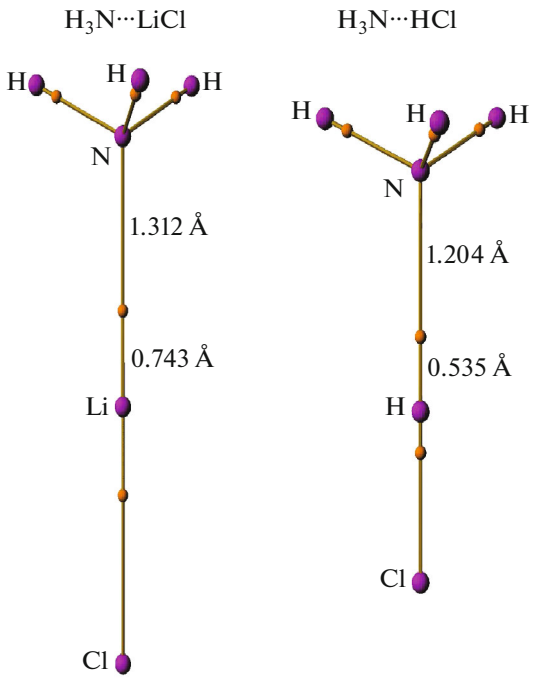

Fig. 5. Molecular graphs of electron density, plotted for complexes $H_3N\cdots LiCl$ and $H_3N\cdots HCl$. Magenta and orange-coloured spheres correspond to critical points (3,−3) and (3, −1), respectively; the brown lines denote the bond paths. The numbers indicate the distance (in Å) from the nucleus to the bond critical point (3, −1) of intermolecular contact N···Li and N···H.

Table 3. Electron density (ρ), Laplacian of electron density ($\nabla^2\rho$), potential energy density (V_{BCP}), total energy density (H_{BCP}), parameters of the localization of electrons (ELF) and orbitals (LOL), and electrostatic potential (ESP) at the critical point of intermolecular contact in the lithium- and hydrogen-bonded complexes

Molecular complex	Topological parameters				ELF	LOL	ESP
	ρ	$\nabla^2\rho$	V_{BCP}	H_{BCP}			
Complex A: lithium bonds							
$H_3N\cdots LiF$	0.0257	0.1626	−0.0285	0.0061	0.0334	0.1567	0.3002
$H_3N\cdots LiCl$	0.0276	0.1767	−0.0313	0.0065	0.0353	0.1606	0.3319
$H_3N\cdots LiBr$	0.0283	0.1822	−0.0325	0.0065	0.0361	0.1623	0.3403
$H_3N\cdots LiH$	0.0264	0.1687	−0.0296	0.0063	0.0340	0.1581	0.3083
Complex B: hydrogen bonds							
$H_3N\cdots HF$	0.0531	0.0805	−0.0536	−0.0167	0.2546	0.3689	0.3572
$H_3N\cdots HCl$	0.0506	0.0693	−0.0464	−0.0145	0.2802	0.3843	0.2781
$H_3N\cdots HBr$	0.0586	0.0570	−0.0552	−0.0205	0.3479	0.4222	0.3081

All values are in atomic units. Table 3 does not include ellipticity ε of the Laplacian because its calculated values at the critical point are less than 0.001.

Table 4. Nonbonded (r^0) and bonded (r) radii of nitrogen and lithium (hydrogen) atoms, and their mutual penetration (Δr) (Å) in the formation of lithium- and hydrogen-bonded complexes

Molecular complex	r^0_{Li}/r^0_H	r_{Li}/r_H	$\Delta r_{Li}/\Delta r_H$	r^0_N	r_N	Δr_N	$\Delta r_{Li}/\Delta r_H + \Delta r_N$
Complex A: lithium bonds							
$H_3N\cdots LiF$	1.116	0.756	0.360	1.810	1.326	0.484	0.844
$H_3N\cdots LiCl$	1.188	0.743	0.445	1.809	1.312	0.497	0.942
$H_3N\cdots LiBr$	1.219	0.739	0.480	1.809	1.305	0.504	0.984
$H_3N\cdots LiH$	1.283	0.750	0.533	1.811	1.319	0.492	1.025
Complex B: hydrogen bonds							
$H_3N\cdots HF$	1.475	0.487	0.988	1.799	1.194	0.605	1.593
$H_3N\cdots HCl$	1.585	0.535	1.050	1.801	1.204	0.597	1.647
$H_3N\cdots HBr$	1.620	0.515	1.105	1.798	1.173	0.625	1.730

Mutual penetration of atoms of intermolecular contact was determined according to relation $\Delta r = r^0 - r$.

electron density near the hydrogen atom that participates in H-bonding in complex $H_3N\cdots HCl$ (indicated in green) is thus very great and more than the increase on the nitrogen atom of ammonia (indicated in violet on the line of hydrogen bond). We see the opposite picture on the line of the intermolecular bond between nitrogen and lithium in the complex $H_3N\cdots LiCl$: a negligible reduction of electron density in the region adjacent to the lithium atom, and a very strong increase of it near the nitrogen atom.

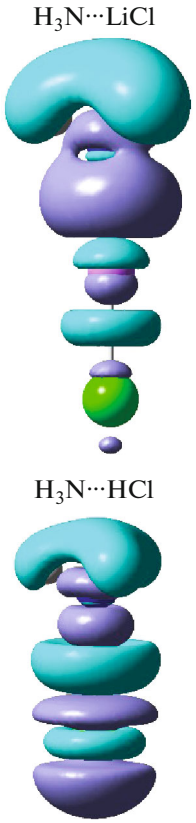

Fig. 6. Maps of the electron density redistribution for complexes $H_3N\cdots LiCl$ and $H_3N\cdots HCl$, plotted according to MP2/aug-cc-pVTZ calculations; the border of the contour runs along the 0.0005 a.u. isoline. Blue color indicates increase of electron density, while green color indicates its loss at formation of the molecular complex from monomers.

Decomposing Binding Energy into Components

Information on the nature of intermolecular bonds can be obtained on the basis of data on components of the energy of interaction between the monomers that forming a complex. Analysis of intermolecular energy according to the Morokuma–Kitaura scheme [55], results from which are presented in Table 5 for complexes A and B, can be used to answer the question of whether the higher stability of complexes with Li bonds is determined only by electrostatic interaction. Decomposing the binding energy into components using Dunning's basis set aug-cc-pVTZ and Pople's basis set 6-311++G(3*df*,3*pd*) reveals that the type of the basis set has a very low impact on the calculated magnitudes of the components without changing the full picture of the intermolecular interaction.

A comparison of the electrostatic contributions (the ES component) to the binding energy in complexes A and B shows that the ES component in the complexes with Li bonds is a bit larger than in the H-bonded complexes. The energy of polarization (POL) proved to be the second largest component in the A-complexes. The contribution from polarization to the energy of Li bonds grows rapidly in the order $H_3N\cdots LiF < H_3N\cdots LiCl < H_3N\cdots LiBr$ and apparently determines the increased stability of the complex with heavy halogen. On the other hand, the value of the POL component falls slightly in complexes with H bonds upon moving to heavy atoms.

Table 5. Components of binding energy (kcal/mol) in lithium- and hydrogen-bonded complexes, obtained with the Morokuma–Kitaura scheme

Molecular complex	Components of binding energy				
	ES	EX	POL	CT	DISP
Complex A: lithium bonds					
$H_3N\cdots LiF$	−25.91 (−26.41)	10.83 (10.59)	−9.93 (−9.64)	−3.16 (−2.92)	0.36 (0.31)
$H_3N\cdots LiCl$	−28.28 (−29.31)	11.79 (11.53)	−12.28 (−11.85)	−3.81 (−3.47)	0.40 (0.38)
$H_3N\cdots LiBr$	−30.81 (−31.22)	13.18 (12.78)	−25.80 (−25.19)	−2.49 (−2.14)	−0.03 (−0.05)
$H_3N\cdots LiH$	−26.51 (−27.13)	11.36 (11.15)	−29.32 (−29.01)	−3.05 (−2.95)	0.58 (0.54)
Complex B: hydrogen bonds					
$H_3N\cdots HF$	−23.34 (−23.85)	22.56 (22.37)	−9.63 (−9.47)	−9.55 (−9.06)	−2.98 (−3.19)
$H_3N\cdots HCl$	−20.98 (−21.23)	27.59 (27.12)	−9.16 (−8.96)	−12.48 (−11.84)	−3.86 (−4.05)
$H_3N\cdots HBr$	−23.61 (−23.94)	34.10 (33.52)	−9.01 (−8.78)	−15.14 (−14.22)	−4.73 (−4.85)

ES, EX, POL, and CT are components of electrostatic interaction, exchange repulsion, polarization, and charge transfer, respectively. Components with a negative sign are attractive. Table 5 does not include the MIX component of the Morokuma–Kitaura decomposition. DISP is the energy of dispersion, assumed to equal the calculated energy of electron correlation. Values of components calculated with basis set 6-311++G(3*df*,3*pd*) are in parentheses.

It is clear from the data in the Table 5 that the value of the ES component varies slightly in the H-bonded complexes, which prevents bonding at the higher binding energy in complex $H_3N\cdots HF$ with its stronger electrostatic interaction. According to our analysis, the drop in binding energy in the H-bonded complex with the larger and less electronegative halogen atom is determined by the rapid growth of the exchange repulsion (EX) of monomers. In complexes $H_3N\cdots HCl$ and $H_3N\cdots HBr$, the EX component is much greater than electrostatic contribution to the energy of H bonds. In the A-complexes, it varies from 41.3 to 42.9% of the ES component, according to calculations with the aug-cc-pVTZ basis set.

Note too the difference between complexes A and B in the components with charge transfer (CT) and dispersion energy (DISP). The charge transfer makes a relatively small contribution to the Li-bond energy (8 to 13%), but the value of the CT-component in the H-bonded complexes exceeds the contribution of polarization, which grows along with the atomic number and reaches 64% of the ES component in complex $H_3N\cdots HBr$. The values of the energy of dispersion, calculated as energy E_{corr} of electron correlation are given in the last column of Table 5, along with the Morokuma–Kitaura decomposition. The value of E_{corr} is defined as the difference between total energies of the complexes found on the post-SCF and SCF levels of theory. It ranges from 3 to 5 kcal/mol in the B-complexes. In the complexes A, E_{corr} is close to zero and even displays a low positive value. This is consistent with results obtained for Li bonds in [16, 56], where it was revealed that dispersion contributes negligibly to the energy of intermolecular lithium bonds.

CONCLUSIONS

Quantum chemical MP2/aug-cc-pVTZ calculations for complexes formed by ammonia together with molecules LiHal (complexes A) and HHal (complexes B, where Hal = F, Cl, Br) revealed several important differences between their properties and nature of the intermolecular interaction. These differences were apparently due to the different nature of inter-orbital interaction in complexes A and B. According to data from NBO analysis, the main inter-orbital interaction in complexes A is the overlapping of the *n*-orbitals of lone pairs of electrons of nitrogen atoms and the anti-orbitals of lone pairs of lithium atoms, $n_N \rightarrow n^*_{Li}$. In complexes B, the overlapping of the *n*-orbital of nitrogen and the anti-σ-orbital of covalent bond H–Hal ($n_N \rightarrow \sigma^*_{H-Hal}$) makes the main contribution to energy $E(2)$ of inter-orbital interaction.

In complexes A, energy $E(2)$ of inter-orbital interaction rises along with the contribution from the *p*-orbital to the hybrid orbital of the Li atom. In accordance with Bent's rule, this is observed upon moving from the LiHal molecule to the less electronegative halogen. In both types of complexes, the value of $E(2)$ correlates with the charge transferred from the ammonia molecule upon the formation of the molecular complex and the elongation of covalent Li–Hal and H–Hal bonds.

Topological analysis of electron density revealed lower values of it and the density of potential energy at the critical point of intermolecular contact N···Li in complexes A, relative to contact N···H in complexes B. Values of the mutual penetration of nitrogen and lithium atoms that form the intermolecular bond are lower in complexes A, as are the calculated parameters of the localization of electrons and orbitals at the bond

critical point of contact N···Li. In both types of complexes, the binding energy correlates linearly with the maximum value of positive electrostatic potential ESP on the bridge atoms of lithium and hydrogen.

Decomposing the intermolecular energy into components revealed that the lower stability of complexes B relative to complexes A is associated not only with the lower values of the ESP potential on hydrogen atoms and weaker electrostatic interaction, but to a great extent with the much stronger exchange repulsion of monomers upon the formation of the hydrogen-bonded complex. Electrostatic interaction and polarization make the main contribution to stabilizing complexes with lithium bonds, while it comes from electrostatics and charge transfer in complexes B. The rise in the energy of lithium bonding in complexes with heavy halogen is defined as the higher value of the polarization component.

Note that our MP2/6-311++G(3*df*,3*pd*) quantum chemical calculations of complexes A and B using Pople's extended basis set predicted a geometry of the complexes that was similar to the one obtained with MP2/aug-cc-pVTZ calculations, along with similar values of the intermolecular binding energy and components of its decomposition.

FUNDING

This work was supported by ongoing institutional funding. No additional grants to perform or direct this particular research were obtained.

CONFLICT OF INTEREST

The author of this work declares that he has no conflicts of interest.

REFERENCES

1. G. Gilli and P. Gilli, *The Nature of the Hydrogen Bond* (Oxford Univ. Press, UK, 2009).
2. E. Peris, J. C. Lee, Jr., J. Rambo, O. Eisenstein, and R. H. Crabtree, J. Am. Chem. Soc. **117**, 3485 (1995).
3. J. Wessel, J. C. Lee, Jr., E. Peris, et al., Angew. Chem. Int. Ed. Engl. **34**, 2507 (1995).
4. P. Metrangolo and G. Resnati, Chem. Eur. J. **7**, 2511 (2001).
5. I. Alkorta, G. Sanchez-Sanz, J. Elguero, and J. E. Del Bene, J. Phys. Chem. A **116**, 2300 (2012).
6. A. N. Isaev, Chem. Phys. Lett. **763**, 138195 (2021).
7. W. Wang, B. Ji, and Y. Zhang, J. Phys. Chem. A **113**, 8132 (2009).
8. A. N. Isaev, Russ. J. Phys. Chem. A **97**, 955 (2023).
9. J. S. Murray, P. Lane, and P. Politzer, Int. J. Quantum Chem. **107**, 2286 (2007).
10. J. E. Del Bene, I. Alkorta, G. Sanchez-Sanz, and J. Elguero, J. Phys. Chem. A **115**, 13724 (2011).
11. S. Scheiner, Int. J. Quantum Chem. **113**, 1609 (2013).
12. J. S. Murray, P. Lane, and P. Politzer, J. Mol. Model. **15**, 723 (2009).
13. S. A. Southern and D. L. Bryce, J. Phys. Chem. A **119**, 11891 (2015).
14. A. Das and E. Arunan, Phys. Chem. Chem. Phys. **25**, 22583 (2023).
15. P. A. Kollman, J. F. Liebman, and L. C. Allen, J. Am. Chem. Soc. **92**, 1142 (1970).
16. Z. Latajka and S. Scheiner, J. Chem. Phys. **81**, 4014 (1984).
17. Z. Latajka, H. Ratajczak, K. Morokuma, and W. J. Orville-Thomas, J. Mol. Struct. **146**, 263 (1986).
18. M. M. Szczęśniak, I. J. Kurnig, and S. Scheiner, J. Chem. Phys. **89**, 3131 (1988).
19. P. Lipkowski and S. J. Grabowski, Chem. Phys. Lett. **591**, 113 (2014).
20. T. Clark, M. Hennemann, J. S. Murray, and P. Politzer, J. Mol. Model. **13**, 291 (2007).
21. P. Politzer, K. E. Riley, F. A. Bulat, and J. S. Murray, Theor. Chem. **998**, 2 (2012).
22. P. Politzer, J. S. Murray, and T. Clark, Phys. Chem. Chem. Phys. **15**, 11178 (2013).
23. G. A. Jeffrey and W. Saenger, *Hydrogen Bonding in Biological Structures* (Springer, Berlin, 1990).
24. P. Kollman, J. Am. Chem. Soc. **99**, 4875 (1977).
25. J. S. Murray, P. Lane, T. Clark, et al., J. Mol. Model. **18**, 541 (2012).
26. S. V. Rosokha and M. K. Vinakos, Phys. Chem. Chem. Phys. **16**, 1809 (2014).
27. L. P. Wolters and F. M. Bickelhaupt, Chem. Open **1**, 96 (2012).
28. K. E. Riley and P. Hobza, J. Chem. Theory Comput. **4**, 232 (2008).
29. P. Deepa, B. V. Pandiyan, P. Kolandaivel, and P. Hobza, Phys. Chem. Chem. Phys. **16**, 2038 (2014).
30. M. J. Frisch, G. W. Trucks, H. B. Schlegel, et al., *Gaussian, 09. Revision D.01* (Gaussian Inc., Wallingford CT, 2009).
31. C. Moller and M. S. Plesset, Phys. Rev. **46**, 618 (1934).
32. R. A. Kendall, T. H. Dunning, Jr., and R. J. Harrison, J. Chem. Phys. **96**, 6796 (1992).
33. M. J. Frisch, J. A. Pople, and J. S. Binkley, J. Chem. Phys. **80**, 3265 (1984).
34. A. E. Reed, F. Weinhold, L. A. Curtiss, and D. J. Pochatko, J. Chem. Phys. **84**, 5687 (1986).
35. A. E. Reed, L. A. Curtiss, and F. Weinhold, Chem. Rev. **88**, 899 (1988).
36. R. Ditchfield, Mol. Phys. **27**, 789 (1974).
37. K. Wolinski, J. F. Hilton, and P. Pulay, J. Am. Chem. Soc. **112**, 8251 (1990).
38. T. Lu and F. Chen, J. Comput. Chem. **33**, 580 (2012).
39. R. F. W. Bader, Chem. Rev. **91**, 893 (1991).
40. R. F. W. Bader, *Atoms in Molecules, a Quantum Theory* (Clarendon, Oxford, 1993).
41. M. W. Schmidt, K. K. Baldridge, J. A. Boatz, et al., J. Comput. Chem. **14**, 1347 (1993).
42. M. S. Gordon and M. W. Schmidt, in *Theory and Applications of Computational Chemistry: The First Forty Years,* Ed. by C. E. Dykstra, G. Frenking, K. S. Kim,

and G. E. Scuseria (Elsevier, Amsterdam, 2005), p. 1167.

43. S. A. C. McDowell and R. C. Marcellin, J. Chem. Phys. **133**, 144307 (2010).
44. S. A. C. McDowell and J. A. S. S. Hill, J. Chem. Phys. **135**, 164303 (2011).
45. E. Cubero, M. Orozko, and F. Luque, Chem. Phys. Lett. **310**, 445 (1999).
46. W. Qian and S. Krimm, J. Phys. Chem. A **106**, 6628 (2002).
47. I. V. Alabugin, M. Manoharan, S. Peabody, and F. Weinhold, J. Am. Chem. Soc. **125**, 5973 (2003).
48. S. J. Grabowski, J. Phys. Chem. A **115**, 12789 (2011).
49. H. A. Bent, Chem. Rev. **61**, 275 (1961).
50. X. Li, Y. Zeng, X.-Y. Zhang, et al., J. Mol. Model. **17**, 757 (2011).
51. K. Yuan, Y. Liu, L. Lu, et al., Chin. J. Chem. **27**, 697 (2009).
52. O. Mó, M. Yánez, and J. Elguero, J. Mol. Struct.: THEOCHEM **314**, 73 (1994).
53. E. Espinosa, E. Molins, and C. Lecomte, Chem. Phys. Lett. **285**, 170 (1998).
54. D. Cremer and E. Kraka, Angew. Chem., Int. Ed. Engl. **23**, 627 (1984).
55. K. Morokuma and K. Kitaura, in *Molecular Interactions* (Wiley, New York, 1980), p. 21.
56. S. Salai Cheettu Ammal and P. Venuvanalingam, J. Chem. Soc., Faraday Trans. **94**, 2669 (1998).

Translated by G. Levina